

Tunneling spectroscopic analysis of optically active wide band-gap semiconductors

D. A. Bonnell and G. S. Rohrer^{a)}
The University of Pennsylvania, Philadelphia, Pennsylvania 19104

R. H. French
E. I. DuPont de Nemours, Wilmington, Delaware 19880

(Received 24 July 1990; accepted 15 December 1990)

Tunneling spectroscopy has been used to detect the photoexcitation of charge carriers in the wide band-gap semiconductors, ZnO and cubic SiC. Because the process is energy sensitive, valence-to-conduction band or defect charge transfer transitions may be selectively excited and detected with the scanning tunneling microscope. Two types of transitions were detected which change the tunneling response; for cubic SiC valence-to-conduction band transitions were excited, while for Co^{2+} and Mn^{2+} doped ZnO electron charge transfer transitions from the dopants to the conduction bands occur. Preliminary results on the effect of a continuous energy (ultraviolet) light source on the tunneling spectrum of ZnO are presented.

I. INTRODUCTION

Monochromatic light sources have previously been used in conjunction with scanning tunneling microscopy (STM) to modulate the sample-tip separation through local heating,¹ to increase conductance in semi-insulating GaAs² and to examine the surface photovoltage effect on the Si (111) (7×7) surface.³ Although not explicit in this previous work, detection of photoexcitation in tunneling spectroscopy should not, in principle, be limited to narrow band-gap semiconductors or to valence-to-conduction band transitions. Optically active defect states resulting from elements in solid solution or from structural defects should also be observable. In addition, the combination of the high energy resolution of optical spectroscopy with the high spatial resolution of STM would provide considerable insight into problems involving the electronic structure of defects in solids. The paper presents the first observations probing subsurface chemical defects using tunneling spectroscopy augmented by optical excitation in materials with band gaps as large as 3.2 eV.

In STM analysis of wide band-gap semiconductors one of two conditions obtains, either a high density of surface states pins the surface Fermi level as in the case of most STM analyses or a Schottky barrier forms.^{4,5} In either case, the bulk energy bands are bent and a depletion layer forms under the probe tip which can 'pinch'-off the tunnel current as has been demonstrated by Feenstra *et al.* on GaAs.⁶ The width of the depletion layer decreases as the carrier concentration increases, and, therefore, could be altered by photoexcitation. A band-to-band excitation will typically create a pair of mobile carriers which will drift in different directions in the depletion layer field gradient, while a charge transfer transition of an electron to the conduction band or a hole to the valence band will create one free-carrier which can move in the field. The increased carrier concentration will cause a reduction in band bending, since the depletion layer depth is inversely proportional to the square root of the charge carrier density, and should be detected in the STM as a change

in local capacitance, in conductance at constant sample-tip separation or in tunnel barrier height.

The two possible types of excitation, valence-to-conduction band transition, and charge transfer excitation, are considered separately here. To explore the first, hexagonal SiC and cubic SiC were examined during illumination with 2.81 eV light. Due to the differences in band-gap energies, valence-to-conduction band transitions should be allowed for cubic SiC but not for hexagonal SiC. To observe the second type of excitation undoped ZnO and ZnO doped with Co^{2+} and Mn^{2+} were examined under the same illumination. In this situation, transitions from the Co^{2+} and Mn^{2+} levels to the conduction band are allowed while valence-to-conduction band transitions are forbidden. After a description of the experimental procedures and sample preparation, electronic structure of the samples as determined by optical spectroscopy are presented, then tunneling spectra with and without illumination are compared. Observations are discussed in terms of the effects of optical excitations on the tunneling spectra.

II. EXPERIMENTAL PROCEDURE

Scanning tunneling microscopy was carried out in ultra-high-vacuum (UHV) with a base pressure $< 5\times 10^{-10}$ Torr. The microscope used in these experiments was of a standard design, described in detail elsewhere,⁷ and the tips were formed mechanically from 0.01 in. Pt wire. Samples were attached to silver or copper plates using silver print. The chamber was configured such that the sample-tip junction could be illuminated by an external light source. The light source was a He-Cd laser which produces a 7 mW beam of 441.6 nm, 2.81 eV light. Photon flux reaching the sample is estimated at 1.5×10^{16} /s. Current-voltage (I - V) curves were acquired over an energy range of 6 eV using the interrupted-feedback (100–300 μms) method in the presence and absence of illumination at a variety of sample-tip separations. Each I - V curve is an average of between 10 and 32

curves which were acquired sequentially. Since a small variation in sample-tip separation during acquisition of a spectrum will result in an apparent change in local conductance, several steps were taken to characterize the stability of the tunnel junction. The junction was brought to thermal equilibrium while under feedback control so that further expansion did not occur during the measurement. Drift during the feedback interrupt was negligible. Ten series of spectra were acquired in the illuminated condition after which ten were acquired in the nonilluminated condition. These measurements were compared with a series of alternating illuminated/nonilluminated measurements. The entire sequence was repeated over four times on at least 5 different days for each sample. While the magnitude of the conductance did vary somewhat due to tip instability and the angle of the impinging radiation, the relative differences reported here were consistent in every measurement.

Transmission and reflectance measurements were performed on the SiC using a Perkin Elmer Lambda-9 UV-Vis spectrophotometer, and the absorption coefficient, α in units of cm^{-1} , determined using a 2-D Newton's method which corrects for multiple internal reflectance losses in the sample.⁸ The band-gap energy of a bulk material can be experimentally determined from the bulk absorption coefficient by a fitting procedure where either a direct or indirect band-gap model is presumed. The absorption depth, d , of the photon flux can be determined from the absorption coefficient by the condition $\alpha d = 1$ and determines the volume of the sample in which the incident photons will excite charge carriers.

Four samples were examined, a cubic SiC crystal, a hexagonal SiC single crystal, a ZnO single crystal, and doped polycrystalline ZnO. The cubic SiC crystal, grown by chemical vapor deposition methods (CVD), was a transparent crystal 20- μm thick with a yellowish color.⁹ The green, transparent, hexagonal SiC crystal, grown by the Acheson process, was 450- μm thick and was presumably of mixed polytypes. Nearly intrinsic, transparent, colorless, single-crystal ZnO was annealed at 500 °C in a zinc overpressure to introduce a population of shallow donors. The electronic conductivity of the crystal increased and it became orange in color as a result of the reduction. The doped ZnO sample was prepared via chemical methods¹⁰ and contains 0.1% CoO, 0.1% MnO 0.1% Bi_2O_3 and 150 ppm Al_2O_3 . The defect chemistry of this sample has been rather well characterized^{11,12} and is summarized in Table I. Note that the tetrahedrally coordinated transition elements, Mn and Co, induce defect states 1.9 eV below the conduction band edge. A number of energies have been reported for the shallow defects states, i.e., singly and doubly ionized oxygen vacancies and zinc interstitials. Representative values are provided in Table I, the important point being that the shallow donors will be ionized at room temperature and will not contribute additional charge carriers during illumination.

It is well known that the electronic structure of ZnO surfaces is affected by atmospheric gases which can be adsorbed on the surface.¹³ In order to eliminate any effects of photo-desorption the doped ZnO sample was cleaned *in situ*. After polishing and cleaning in acetone and ethanol, the sample was heated in air to 140 °C for 30 min, then to 500 °C for 30

TABLE I. Excitations observed in tunneling response

Sample	Relevant energies ^a	Under illumination
ZnO single crystal	3.24 eV (band gap) 0.32 eV (O vacancy) 0.03 eV (Zn interstitial)	no effect
ZnO, doped	3.24 eV (band gap) 1.92 eV (tet. Co^{2+}) 1.92 eV (tet. Mn^{2+}) 0.32 eV (O vacancy) 0.03 eV (Zn interstitial)	increased conductance
SiC, hexagonal	2.79 eV (band gap)	no effect
SiC, cubic	2.51 eV (band gap)	increased conductance

^a Except for the band gaps these energies are referenced from the bottom of the conduction band

min and finally was heated to 400 °C for 10 min in vacuum to remove any chemisorbed gases. The composition of residual gases in the chamber was monitored before, during and after laser illumination. (A controlled study of the effects of adsorption of CO_2 , O_2 and H_2O in the tunneling spectra of ZnO polar and nonpolar surfaces will be reported elsewhere.¹⁴)

III. RESULTS

The electronic structure of the samples will determine their interaction with the laser illumination, and the method and efficiency of induced charge carrier creation. For intrinsic band-to-band excitations the important consideration is the band-gap energy (E_g) and the absorption coefficient of the crystals at the laser photon energy. For charge transfer excitations, the donor-to-conduction band energy difference and the absorption coefficient of this transition at 2.81 eV will dictate the efficiency of charge carrier creation. As shown in Fig. 1, the cubic SiC sample has a direct gap energy

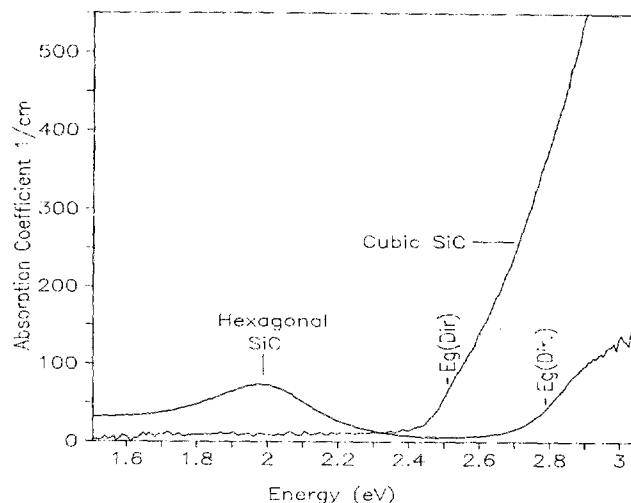


FIG. 1. Optical absorption spectra of cubic and hexagonal SiC.

of 2.51 eV for fitting $75 < a < 150 \text{ cm}^{-1}$, while the hexagonal SiC sample has a direct gap energy of 2.79 eV fitted in the same range of α . For the cubic SiC the absorption coefficient at 2.81 eV is 410 cm^{-1} while for the hexagonal SiC it is only 56 cm^{-1} . There is roughly a factor of 10 increase in the volume over which the laser excites charge carriers in the hexagonal SiC sample and, therefore, a factor of 10 decrease in this sample's charge carrier increase under illumination compared to the cubic SiC sample. The hexagonal SiC sample also exhibits a defect absorption at 2.0 eV (visible in Fig. 1) arising from a transition which will not contribute a charge carrier.

No photoconduction effect was observed in the tunneling spectra or in the current on sample-tip contact in the analysis of the hexagonal SiC crystal in air, where the effect usually appears to be most pronounced; consequently, this sample was not analyzed in UHV. The results of the analysis of cubic SiC are illustrated in the current-voltage curves and derivative spectra of Fig. 2. Illumination of the junction in air increased the conduction above the Fermi level. In this case the increased conductance must result from valence-to-conduction band transitions. This is similar to the result of van

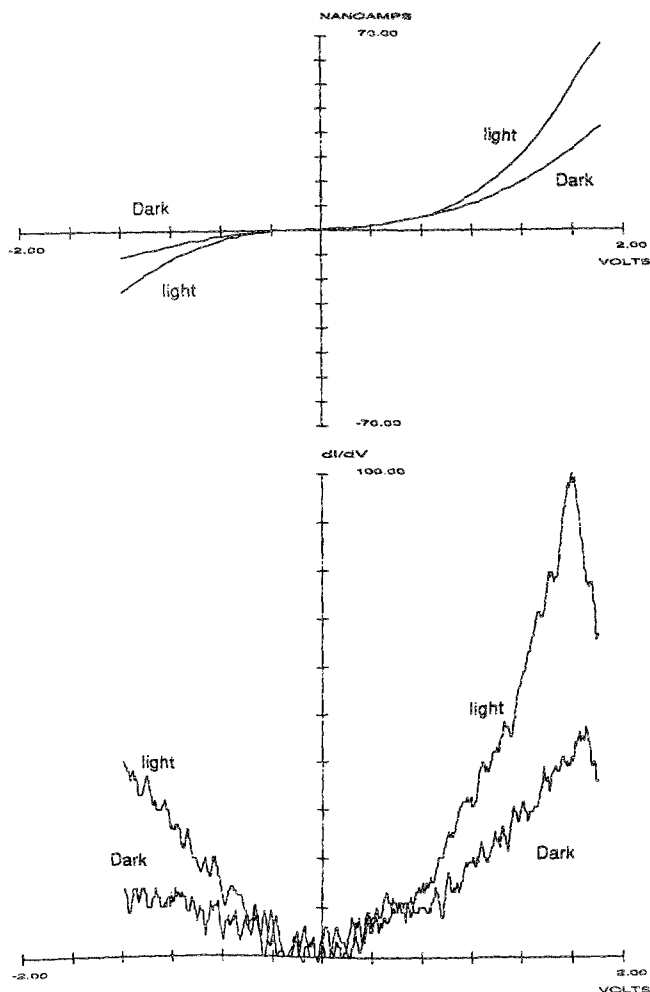


FIG. 2. A comparison of the tunneling spectra of cubic SiC in vacuum in the presence and absence of illumination; acquired at 1.0 V and 6.0 nA.

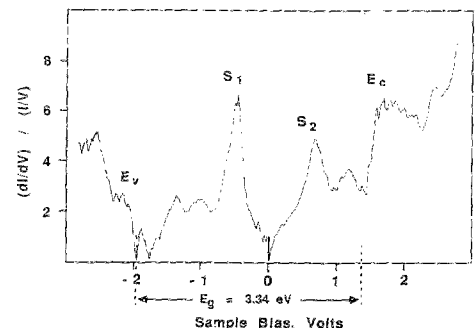
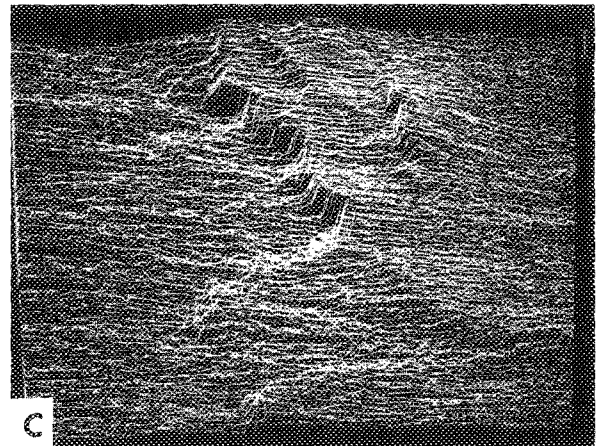
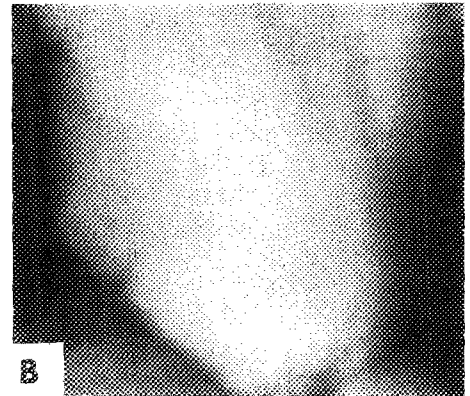
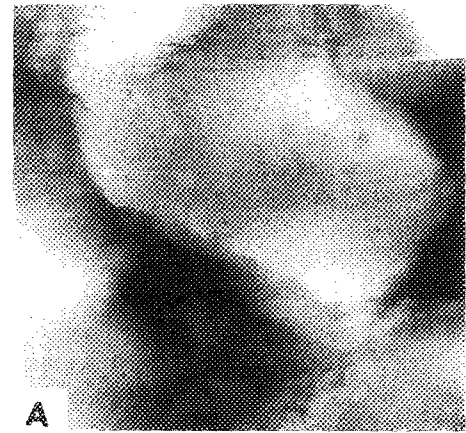


FIG. 3. Constant current images (a) of $4950 \times 4950 \text{ \AA}$ area of doped ZnO acquired at 0.5 nA, -2.75 V , full vertical scale 700 \AA , (b) $5500 \times 5500 \text{ \AA}$ area acquired at 0.5 nA, -3.0 V with full vertical scale 760 \AA , (c) $137 \times 137 \text{ \AA}$ area acquired at 0.2 nA, -1.5 V , vertical marker indicates 14 \AA , and (d) the tunneling spectrum indicating the valence band edge, E_v , the conduction band edge, E_c , and two midgap states, S_1 and S_2 . This structure is common on the doped sample and is typical of the ZnO (1010) surface.

de Walle *et al.* except that SiC has a band gap larger than GaAs by a factor of 2 and we have also tested the null case in which the band-gap energy is larger than the energy of the photons.

ZnO surfaces usually contain a number of steps. The step density and dimension of the facets varies as is illustrated in the image of the undoped sample shown in Fig. 3. No effect in the tunneling behavior was observed on illumination of the undoped sample; a reasonable result as a large density of bulk defect states is not present in the forbidden gap and the light has insufficient energy to induce valence-to-conduction band excitations. The electronic structure typical of doped ZnO is shown in Fig. 4. The features common to all regions of the sample are the valence band edge, E_v , the conduction band edge, E_c , and two midgap states, S_1 and S_2 . The remaining details of the spectrum varied with position. This structure is also typical of the ZnO (1010) nonpolar face of the undoped crystal. In contrast to the undoped sample, the ZnO containing transition metal ions exhibited an increased conductance both above and below the Fermi level as shown in Fig. 5. The increased conduction is consistent with the increased carrier concentration that would be produced by

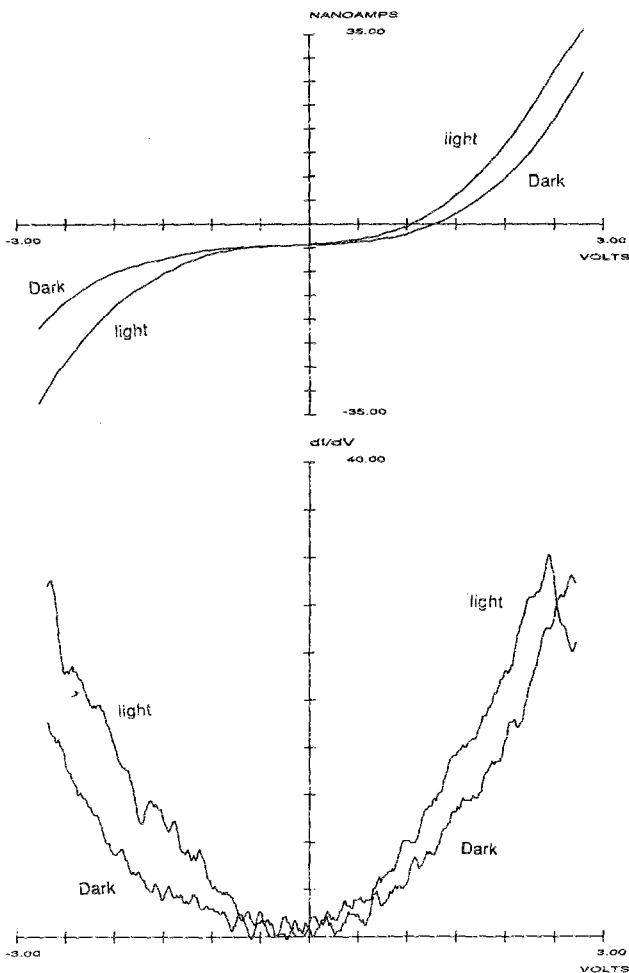


FIG. 4. A comparison of the tunneling spectra of doped ZnO in vacuum in the presence and absence of illumination; acquired at ± 1.0 V and 1.0 nA.

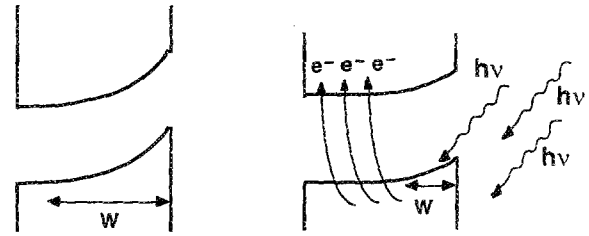


FIG. 5. Schematic diagram of the effect of optical absorption on the depletion depth of a semiconductor exhibiting band bending.

the elevation of electrons from the Co^{2+} and/or Mn^{2+} ground states to the conduction band. The conditions under which excitations were, and were not, observed in the tunneling behavior are summarized in Table I.

IV. DISCUSSION

Except for the possibility of photodesorption, which is discussed in detail below, there are two types of observations that might be expected in the tunneling spectra upon illumination of optically active material. The first involves detailed variations in the positions of band edges due to the change of occupation on optical absorption. Making the most liberal estimate of this occupation change near the valence band edge on excitation by using a beam size of 1 mm, assuming the maximum number of carriers are excited, the fraction of the time spent in excited state is high, and given an absorption depth of $1 \mu\text{m}$, the largest possible value of occupation change, $\Delta n/n$, is about $(1 \times 10^{16}) / (1 \times 10^{18})$ or about 0.01. Given the restrictive assumptions made in this calculation a more realistic estimate is at least an order of magnitude lower, or 0.01%. A change on this order is not likely to be observable as a change in band edge position in a tunneling spectrum. In the case of charge transfer excitations Δn is about 5×10^{15} , where the number of photons is larger than

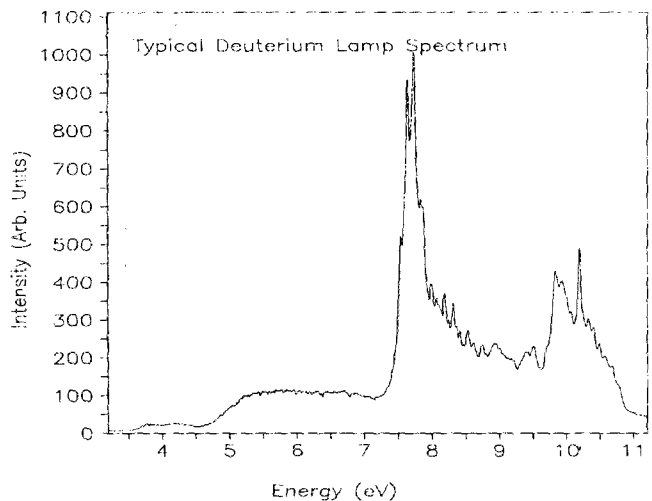


FIG. 6. Energy spectrum of the deuterium light source with relatively high intensities above 5 eV and peaks at 7.5, 7.7, and 9.8 eV.

the concentration of dopants in the ZnO for example. Since none of these states are excited in the absence of illumination, this corresponds to a significant change in occupation of midgap defect states that should be detectable in the tunneling spectrum. We have not observed this effect to date.

The second mechanism involves the dependence of the depletion layer on carrier concentration and is illustrated in Fig. 6. In both the case of valence-to-conduction band transitions and of charge transfer excitations the depletion depth will decrease on optical absorption with a square root dependence on the number of excitations. This will result in an overall increase in local conductance. This mechanism is consistent with the data presented in Figs. 2 and 4; however, our results do not imply that it will not be possible to detect variations of midgap electronic structure.

The adsorption of atmospheric gases on ZnO creates a depletion layer at the surface; therefore, an alternative explanation for the increase in conductance on illumination is that the light stimulates the photodesorption of molecular species from the ZnO surface and causes a reduction in the depletion layer width and increased conductance. There are three reasons why it is unlikely that this process occurs in these experiments. Shapira *et al.* studied photodesorption from ZnO surfaces and found that desorption was only stimulated by photons with energies near or above the band gap.¹⁵ The light used in the current study is in an energy range where almost no detectable desorption occurred in the previous work. This is supported by the observation that there was no detectable change in the residual gas composition of the UHV chamber during the laser illumination of ZnO. Second, the same desorption process should have occurred on both the pure and the doped material, yet the photoexcitation effect was detected only in the doped material. Last, the effect would not have been reproducible in vacuum since the prolonged laser irradiations would have degassed the sample surface. It should also be noted that the small increase in sample temperature associated with the illumination is not enough to drastically change the sample conductance and would have had the same effect on all of the samples.

The potential of combined STM and photoexcitation to realize spatially resolved optical spectroscopy has been demonstrated in this study. The obvious extension of the work utilizing monochromatic radiation is to use a continuous light source. In order to explore this approach, we have used an ultraviolet light source with the characteristics shown in Fig. 6, which is particularly appropriate for wide band-gap semiconductors due to its high intensity above 5 eV. The effects of illumination of ZnO with this source are presented in Fig. 7. Upon illumination several events occur. A photocurrent is emitted which is superimposed on the tunneling signal. This implies that the sample-tip separation has increased and local conductance should decrease if the electronic structure of the sample is not altered by illumination. This is contrary to the experimental observation that there is an increase in density of states near the Fermi level on excitation with a continuous radiation source. Although this is a complex result in that the measured electronic structure contains excited states, the potential to use this approach to

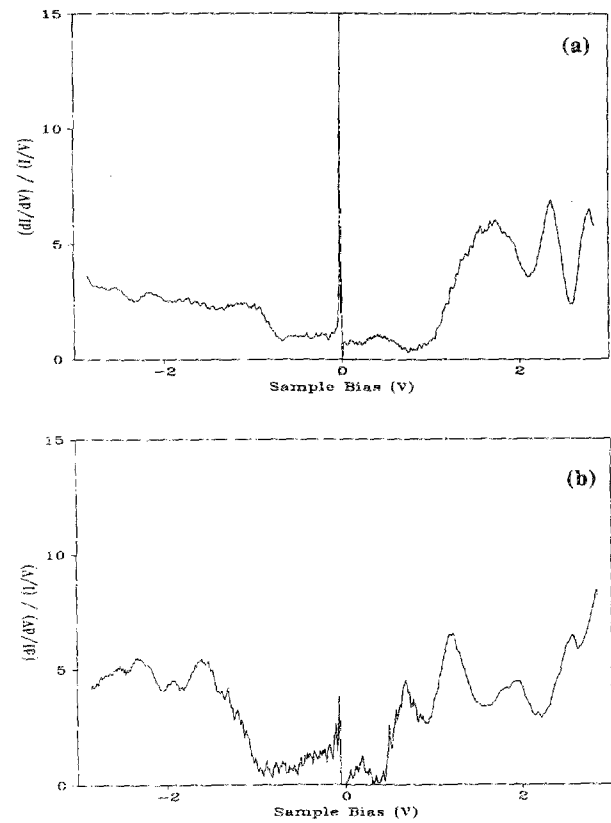


FIG. 7. A comparison of the tunneling spectra of ZnO in the presence (a) and absence (b) of illumination by the deuterium lamp; acquired at -3.0 eV and 17.5 nA.

isolate excitations is obvious. Further work involving systematic measurements using a monochromator with this light source are necessary to be able to understand this behavior.

V. CONCLUSIONS

Valence-to-conduction band transitions in SiC have been observed in tunneling spectra acquired in a STM. In the case of doped ZnO, the charge carrier concentration and tunnel current are increased by the excitation of charge transfer transitions from bulk donor defect states to the conduction bands, thus allowing the STM to probe subsurface chemical defects. The energy sensitivity of the process suggests that the tunneling current may be used as a detector for optical spectroscopy with the high spatial resolution of the STM, an exciting development with the potential of identifying microscopic structural and chemical defects. Progress towards this end has been demonstrated in preliminary observations of multiple excitations in ZnO from a continuous energy light source in the tunneling current.

ACKNOWLEDGMENTS

We are grateful to G. Pike for providing ZnO samples, to R. F. Davies for providing the SiC single-crystal films, and to J. Vohs for valuable discussions and for providing a ZnO single crystal. D. A. B. acknowledges support from IBM

Research and the National Science Foundation through the Presidential Young Investigators Program.

^{a)} Current address: Carnegie Mellon University, Department of Metallurgical Engineering and Materials Science, Pittsburgh, PA 15213.

¹ N. M. Amer, A. Skumanich, and D. Ripple, *Appl. Phys. Lett.* **49**, 137 (1986).

² G. F. A. van de Walle, H. van Kempen, P. Wyder, and P. Davidsson, *Appl. Phys. Lett.* **50**, 22 (1987).

³ R. J. Hamers and K. Markert *Phys. Rev. Lett.* **64**, 1051 (1990).

⁴ D. A. Bonnell *Ceram. Trans.* **5**, 315 (1989).

⁵ D. A. Bonnell, *Mater. Sci. Eng. A* **105/106**, 55 (1988).

⁶ R. M. Feenstra and Joseph A. Stroscio, *J. Vac. Sci. Technol. B* **5**, 923 (1987).

⁷ D. A. Bonnell and D. R. Clarke, *J. Am. Ceram. Soc.* **71**, 629 (1988).

⁸ M. E. Innocenzi, R. T. Swimm, M. Bass, R. H. French, A. B. Villaverde, and M. R. Kokta, *J. Appl. Phys.* **67**, 7542 (1990).

⁹ H. P. Liaw and R. F. Davis, *J. Electrochem. Soc.* **132**, 642 (1985).

¹⁰ R. G. Dosch, B. A. Tuttle, and R. A. Brooks, *J. Mater. Res.* **1**, 90 (1986).

¹¹ R. Pappalardo, D. L. Wood, and R. C. Liars, Jr., *J. Chem. Phys.* **35**, 2041 (1961).

¹² A. Smith, J.-F. Baumard, P. Abelard, and M.-F. Denanot, *J. Appl. Phys.* **65**, 5119 (1989).

¹³ W. Gopel, *Prog. Surf. Sci.* **20**, 9 (1985).

¹⁴ G. S. Rohrer and D. Bonnell (unpublished).

¹⁵ Y. Shapira, S. M. Cox, and David Lichtman, *Surf. Sci.* **54**, 43 (1976).